Indian Journal of Chemistry
Vol. 59A, August 2020, pp. 1067-1075

Zirconia-chitosan beads as highly efficient adsorbent for defluoridation of water

Swati Tandekar[a], D. Saravanan[b] & Ravin Jugade[a]*

[a]Department of Chemistry, R.T.M. Nagpur University, Nagpur-440033, India
[b]Department of Chemistry, National College, Tiruchirappalli-620001, India
E-mail: ravinj2001@yahoo.co.in

Received 12 July 2019; revised and accepted 15 June 2020

Zirconia modified chitosan beads (Zr-CTS) have been synthesized as adsorbent for fluoride ions from water bodies. The beads have been characterized using FTIR, SEM, EDX, TG-DTA and BET surface area analysis. Batch adsorption parameters are performed for defluoridation of water using the prepared composite. The pH point of zero charge was found to be 5.7. Maximum efficiency of the adsorbent is observed at pH 4.0, with adsorbent dose of 40 mg per 25 mL of 25 ppm fluoride solution and adsorption period of 45 min. Under these conditions, Zr-CTS is found to have an adsorption capacity of 52.63 mg g^{-1} in accordance with Freundlich adsorption isotherm. Thermodynamics parameters reveal that the process of adsorption was spontaneous, exothermic and leading to increase in entropy. The process follows pseudo-second-order kinetics model. The used material is regenerated using 5% NaCl solution and could be reused in multiple cycles adding greener dimension.

Keywords: Chitosan, Zirconium, Adsorption, Defluoridation

Fluoride is an important pollutant as it originates not only from anthropogenic activities but it comes from various rocks and minerals like fluorite, apatite, rock phosphate and topaz[1]. Naturally occurring fluorides in groundwater are a result of the dissolution of fluoride-containing rock minerals by water[2]. Dissolution of mineral rocks and soils in water and wastewater released from semiconductor manufacturing, coal power plants, electroplating, rubber and fertilizer production industries are some of the reasons for increase fluoride concentration in drinking water. Fluorosis is a common problem associated with fluoride contamination of water. Increasing fluoride concentration in water has already become a very serious issue in many countries. UNICEF report shows 17 out of 32 states of India to be fluoride endemic[3].

Various methods of defluoridation of water include chemical precipitation[4], ion-exchange[5], nanofiltration with membrane optimization[6], adsorption[7]. The adsorption method is a widely accepted pollution-removal technique, because of its ease of operation and cost-effectiveness. Fluoride pollution in drinking water and its removal has been critically reviewed and the advantages of adsorption technique have been discussed[8]. The use of adsorbents containing natural polymers, particularly polysaccharides such as chitin and its derivative chitosan have received great attention. Chitosan is a well known biosorbent materials that coordinate metal cations removal by chelation mechanism because of large number of amino and hydroxyl functional groups. Also, due to its cationic behavior in acidic medium, the protonation of amino groups lead to adsorption of metal anions such as chromate, vanadate etc. by ion exchange method. In spite of its abundant application for metal ions adsorption due to presence of amino and hydroxyl groups, the applicability of chitosan compounds is less exploited for sorption of negative ions like fluoride, cyanide, phosphate, nitrate ions etc. This is quite obvious due to its less affection towards these ions in native form. So, some modified forms of chitosan have been used for defluoridation of water. Biocompatibility and biodegradability of chitosan make them effective host matrix for the incorporation of multivalent metal ions as compared to synthetic polymers[9].

A combination of bioproperties of chitosan when combined with fluoride binding capacity of multivalent metal ions leads to large increase in fluoride adsorption capacity. This idea has been exploited by various workers in the recent years who synthesized composites of chitosan with multivalent metal ions or their oxides. The chitosan-praseodymium complex[10], Fe impregnated chitosan[11], chitin-Sn composite[12], cerium immobilized cross-linked chitosan composite[13], chitosan based magnetic

nanocomposite[14] are a few examples of this type of composite. These materials have shown remarkably higher affinity for fluoride and hence, high adsorption capacities. The physical form of the material also matters. Material in the form of beads is easy to handle as well as separate from the water body. Also, the low adsorption capacity of material is an important issue with most of the reported materials. Crosslinking of chitosan with Zr(IV) for defluoridation purpose has been reported[15]. However, the material being amorphous and non-recyclable, its applicability is limited. Present work reports zirconia-chitosan beads as excellent recyclable and reusable adsorbent for defluoridation of water.

Materials and Methods

Materials

All chemicals and reagents used in the current study were of analytical grade and used without further purification. The commercial high density chitosan biopolymer was supplied by Meck Chemicals, Ahmadabad having degree of deacetylation 95% and MW ≈200 kDa determined by viscometric technique. Acetic acid of analytical grade was purchased from Merck, India Ltd., while zirconium oxychloride and ammonia solution were obtained from Loba Chemie Pvt. Ltd., Mumbai. Only polypropylene wares and vials were used for handling fluoride solution while distilled deionized water was used for preparation of all solutions.

Preparation of Zr-CTS beads

In a typical protocol, 1.0 g of chitosan powder was added to 50 mL of 2% acetic acid solution with continuous and constant stirring at room temperature. The stirring was continued for 30 min to avoid clumps formation leading to a thick homogeneous solution. Subsequently, 0.5 g of zirconium oxychloride powder was added and stirring was continued for another 30 min. The chitosan-Zr(IV) solution was allowed to stand for 10 min. The solution was then dripped into 7.0 % ammonia solution using disposable syringe. Golden colour beads having uniform size were observed as shown in Fig. 1. They were filtered and washed several times till the washing showed negative test for chloride ions and has neutral pH. At last, beads were dried at 50 °C for 12 h.

Batch adsorption procedures

Batch adsorption studies were carried out by taking required concentration of fluoride solution (5 – 60 ppm). The pH was adjusted to 4.0 using dilute HCl and NaOH solutions. It was equilibrated with 20 mg of Zr-CTS beads in polypropylene flasks and stirred at 300 rpm for 45 min. The solution was filtered and the concentration of fluoride was determined using ion analyzer Elico model LI 126 connected with fluoride ion selective electrode. The amount of fluoride adsorbed (mg g^{-1}) on the beads can be given by the following equation,

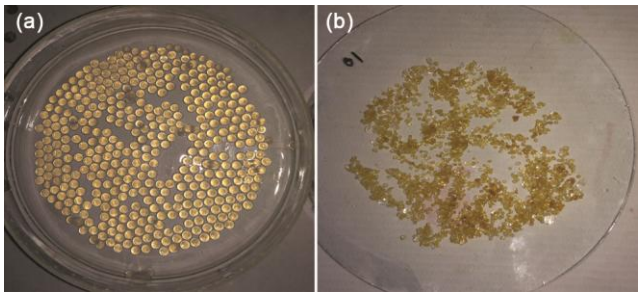

Fig. 1 — Photographs of Zr-CTS beads (a) before and (b) after drying.

$$q_e = \frac{C_0 - C_e}{W} \times V$$

where, C_0 and C_e refer to initial and equilibrated concentration in ppm of fluoride, V is the volume of solution in litre and W is the weight of Zr-CTS beads for adsorption in g. All the experiments were performed three times to check the reproducibility and the mean of three observations have been reported.

Characterization of Zr-CTS beads

It was necessary to characterize the material by various techniques in order to confirm the formation of new composite and to have a clear idea of structural changes that have taken place in the chitosan matrix. The Fourier transform infrared analysis was carried out using FTIR Bruker Alpha, in the wavelength range of 500–4000 cm^{-1}. The surface morphology was imaged by scanning electron microscope (SEM) model Carl Zeiss EVO 18, Germany. EDX studies were carried out simultaneously along with SEM using AMETEK hyphenated to SEM, Zeiss EVO 18. Surface area evaluation was obtained from Brunauer-Emmett-Teller (BET) using conventional analysis by nitrogen adsorption-desorption method on single point surface area analyzer model Smart Sorb 92/93. Thermogravimetric (TG) and differential thermal analysis (DTA) were carried out using Shimadzu DTG 60 model to ascertain the thermal stability of the adsorbent.

Results and Discussion

FTIR spectral characterization

The FTIR spectra of parent chitosan (Fig. 2a) indicates the characteristic absorptions peaks at 3846 cm^{-1} corresponds to the hydroxyl (–OH) stretching band and at 3266 cm^{-1} indicated the existence stretching band of $–NH_2$ group, while –CH group bands appear at 2890 cm^{-1}. The band for N-H bending vibration was visible at 1646 cm^{-1} while that of O-H bending was observed at 1423 cm^{-1}. The sharp band at 1151 cm^{-1} was assigned to the presence of pyranose group of chitosan. The broad band at 1024 cm^{-1} corresponds to the C-O stretching frequency. In Zr-CTS beads, the new peaks observed at 1385 and 1764 cm^{-1} have been assigned to Zr-OH bending vibrations[16]. A shift in position and flattening of O-H and N-H stretching bands near 3300 cm^{-1} indicates the interaction between zirconium with these groups. A new peak at around 530 cm^{-1} corresponds to Zr-O stretching frequency (Fig. 2b).

Morphology and composition of adsorbent

SEM images of the Zr-CTS beads before and after adsorption of ions are shown in Fig. 3 at different resolutions. The bead diameter was observed to be typically less than 1 mm and the surface appeared smooth at low resolution. However, the high resolution images clearly show rough surface with systematic folding pattern. The surface was found to get modified after adsorption of fluoride and the folding pattern has been completely destroyed probably due to univalent fluoride ions that may remove crosslinking in some positions. The distribution of elements in the composite before and after fluoride ion adsorption was recorded in EDX spectra as shown in Fig. 3. The EDX spectrum of native chitosan shows major peaks for C, O and N. Zirconium peak was clearly observed in the Zr-CTS beads with zirconium content of about 6%. A new peak of fluorine was observed along with above peaks after adsorption, which clearly indicates the adsorption of fluoride ions on Zr-CTS.

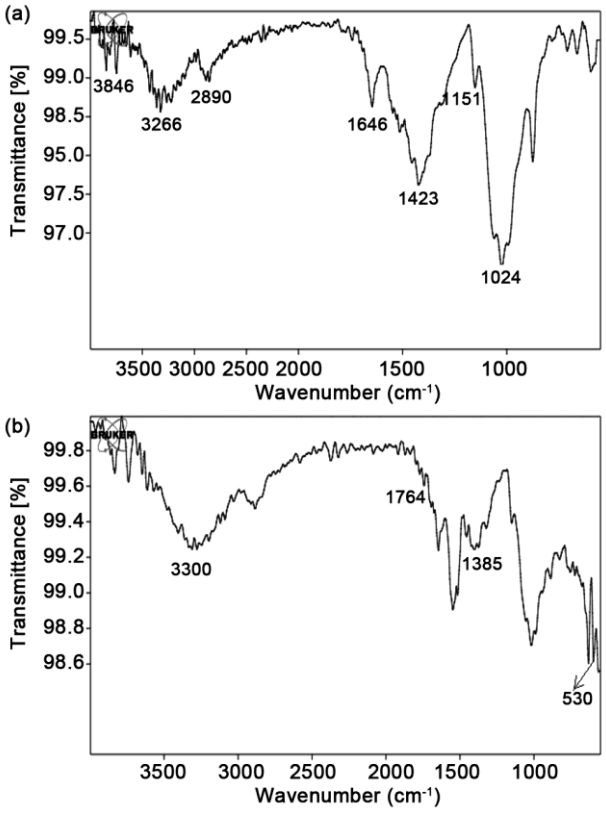

Fig. 2 — FTIR spectra of (a) parent chitosan (b) zirconium modified chitosan beads.

Thermal studies

TG-DTA is a useful characterization that can not only reveal the thermal stability of the new material but also can be used to ascertain the formation of new composite. Also, trapping of any volatile component in the bead can also be revealed from the thermal studies. Thermograms and differential thermograms of native chitosan and Zr-CTS beads have been shown in Fig. 4. Native chitosan shows a two step weight loss. About 5% weight loss around 100 ºC leading to endotherm can be attributed to dehydration. The second weight loss was observed around 300 ºC due to degradation leading to sharp exothermic peak. The thermogram of Zr-CTS beads was found to be entirely different as compared to native chitosan. Initial weight loss around 100 ºC is not very significant while the first significant weight loss was observed at around 200 ºC with exothermic peak in DTA. This shows the degradation of Zr-CTS at lower temperature compared to native chitosan. The complete material was found to degrade at around 400 to 450 ºC with another exotherm in DTA curve. The early degradation of beads at lower temperature compared to chitosan indicates two possibilities: The bonding between metal and chitosan is not that strong and also the metal may catalyze the degradation process.

BET surface area

Surface area of adsorbent is an important parameter as the process of adsorption is surface dependent. However, it is not the only deciding factor for

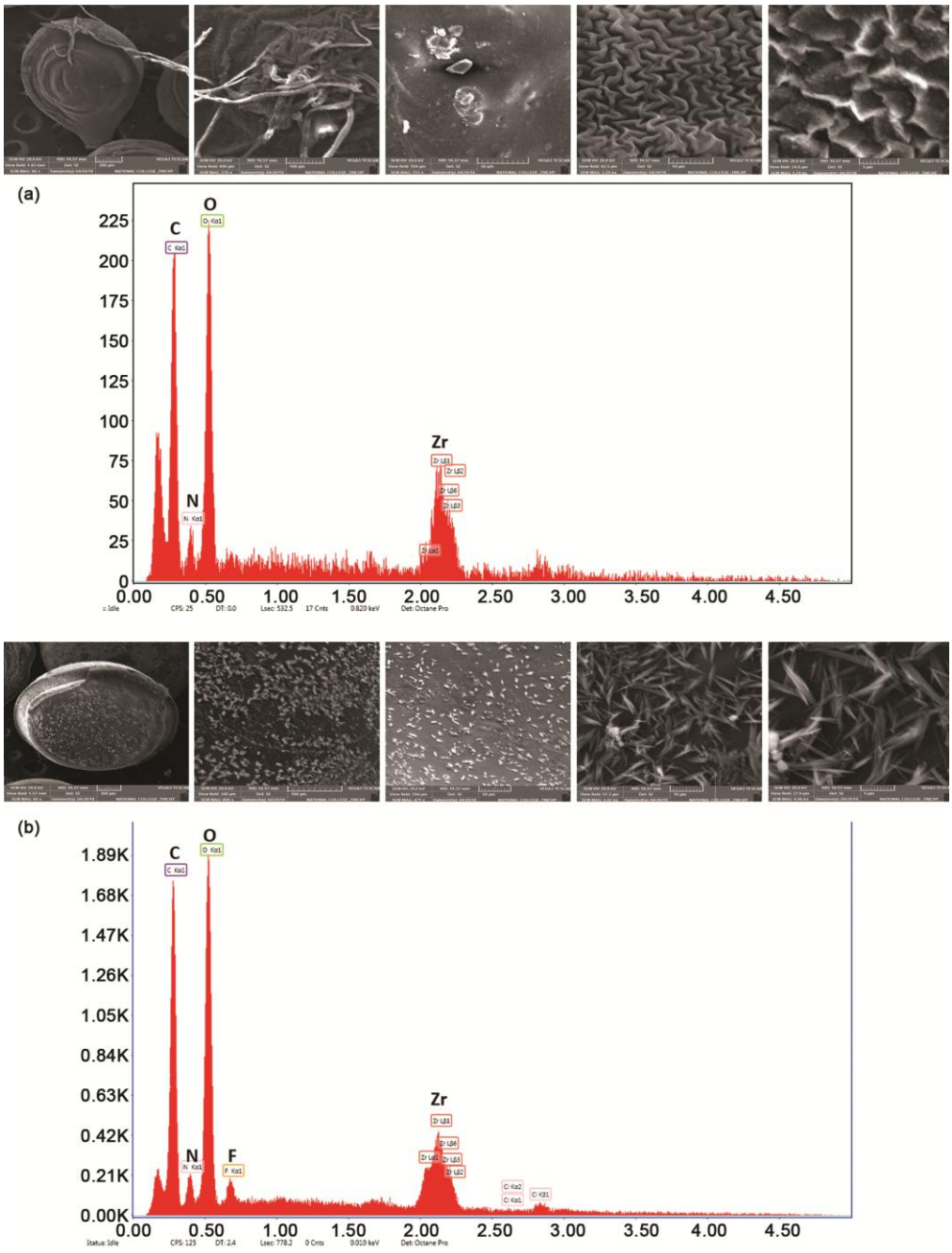

Fig. 3 — SEM images at different resolutions and EDX spectra of zirconium modified chitosan beads: (a) before fluoride ion adsorption and (b) after fluoride ion adsorption.

efficiency of adsorption. The surface area of native chitosan as determined by BET surface area analysis was found to be 0.20 $m^2 g^{-1}$ while that of Zr-CTS beads was found to be 0.14 $m^2 g^{-1}$. The decrease in surface area can be attributed to larger particle size of beads as compared to native chitosan which is in the powdered form.

pH point of zero charge (pH_{PZC})

The pH at the point of zero charge (pH_{PZC}) of the study material was determined by batch equilibrium technique. For this, 50 mL each of 0.1 M NaCl solutions were taken in conical flasks and pH was set from 2.0 to 9.0 using dil. H_2SO_4 and NaOH solutions. To each system, 100 mg of Zr-CTS

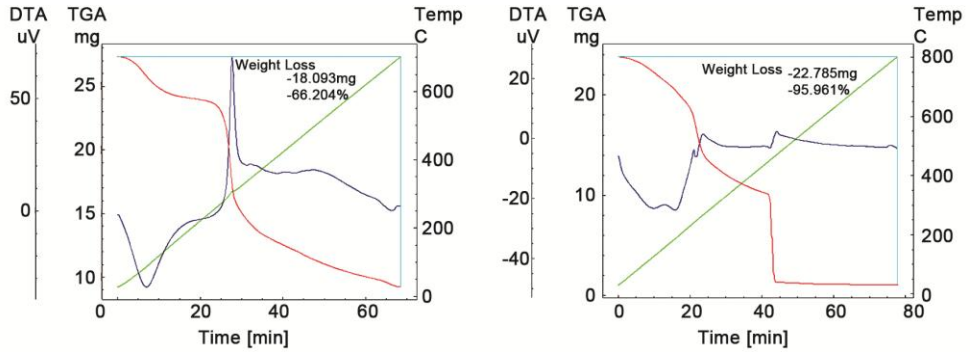

Fig. 4 — Thermogravimetric and differential thermal analysis graphs for (a) native chitosan and (b) Zr-CTS beads.

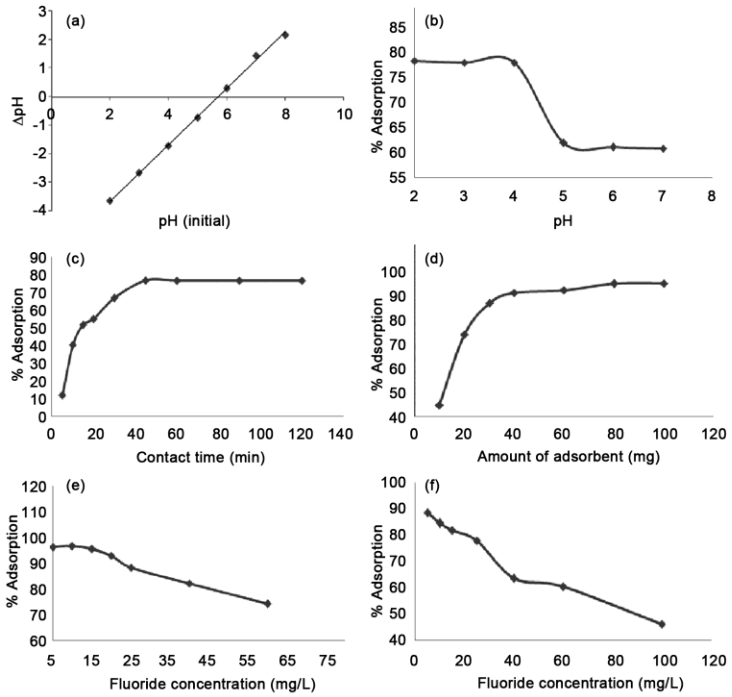

Fig. 5 — Effect of various adsorption parameters on fluoride ion adsorption on zirconium modified chitosan beads: (a) pH_{PZC}, (b) pH, (c) contact time, (d) amount of adsorbent and (e) fluoride ion concentration in batch studies and tea-bag model.

beads were added and the solutions were stirred for 24 h and filtered followed by measurement of the pH. The graph was plotted between changes in pH (ΔpH) as a function of initial pH. The x-intercept gives pH_{PZC} which was found to be 5.7 (Fig. 5a). This indicates that the adsorbent surface charge would be positive below pH 5.7 and it would be negative above pH 5.7.

Effect of pH

The pH of the solution is an important parameter that controls the adsorption at water-adsorbent interface. The pH of solution was varied from 2.0 to 7.0 for various 25 mL 25 ppm solutions of fluoride added with 20 mg of Zr-CTS beads. After stirring for 45 min, the residual concentration of fluoride was determined. The adsorption capacity was found to be maximum and almost constant between pH range of 2.0 to 4.0. Below pH 3.0, the Zr-CTS beads break down during stirring and hence pH 4.0 was fixed for further studies.

Effect of contact time

Effect of contact time on the adsorption of Zr-CTS beads for fluoride concentration 25 mg L^{-1} was studied by varying contact time in the range 5-120 min. The rate of removal of fluoride was found to be higher at the beginning and reaches equilibrium in about 45 min. Therefore, 45 min was fixed as optimum stirring time. (Fig. 5c)

Effect of amount of adsorbent

The effect of Zr-CTS beads was studied by varying the amounts its amount from 10 to 100 mg for same initial fluoride concentration of 25 ppm for equilibration time of 45 min. It was observed that with increase in amount of beads, the percentage of adsorption increases upto 40 mg of beads and then remains constant (Fig. 5d). These are due to the saturation of fluoride ions on the surface of adsorbent. Therefore, amount of adsorbent was fixed as 40 mg.

Effect of fluoride concentration

Effect of initial fluoride concentration on the percentage removal of fluoride was studied by keeping other parameters constant. It was observed that with the increase in fluoride concentration from 5 ppm to 60 ppm, the percentage removal of fluoride decreases slowly (Fig. 5e). This may be because at higher adsorbate concentration, the binding capacity of the adsorbent approaches saturation resulting in decrease in overall percent removal. Hence, 25 ppm fluoride concentration was fixed for all the studies.

In order to use the material for regular defluoridation in household drinking water, tea-bag model[17] is the most useful approach. Hence, the efficiency of Zr-CTS was analyzed for tea-bag experiments. For this, seven systems were prepared with varying concentrations of fluoride from 5 ppm to 60 ppm in different beakers. 40 mg adsorbent was packed in tea bags and suspended into these solutions and stirred for 45 min. The percentage fluoride removal was found to be less than that observed in batch studies. It is quite obvious because in batch studies, there is direct contact between adsorbent and adsorbate. The efficiency of adsorption was found to decrease with increase in fluoride concentration (Fig. 5e). An important advantage of this technique is that it does not require filtration of adsorbent after adsorption is completed.

Adsorption isotherms

Langmuir and Freundlich adsorption isotherms were evaluated to identify the best fitted model for this adsorption. Langmuir isotherm model[18] is used for monolayer adsorption on homogeneous surface. It relates the maximum adsorption capacity (q_o) and the Langmuir isotherm constant (b) which is related to strength of adsorption in linearized form as

$$\frac{C_e}{q_e} = \frac{1}{q_0 b} + \frac{C_e}{q_0}$$

The maximum adsorption capacity q_0 (mg g^{-1}) the constant b (L mg^{-1}) were obtained from the slope and intercept of C_e/q_e against C_e as shown in Fig. 6a.

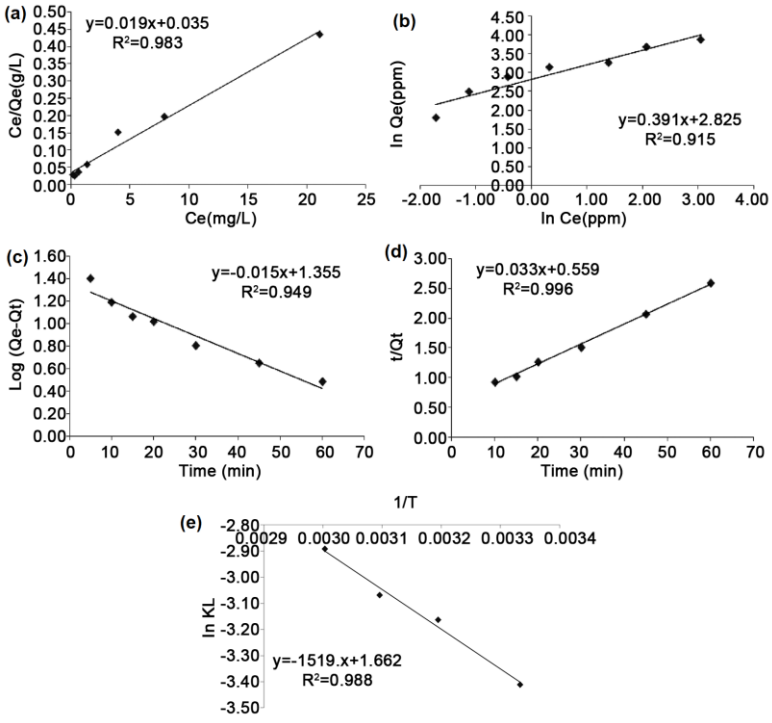

Fig. 6 — Plots for (a) Langmiur isotherm, (b) Freundlich isotherm, (c) pseudo-first order kinetics, (d) pseudo-second order kinetics and (e) vant Hoff's.

Freundlich isotherm model[19] describes the adsorption on non-equivalent sites attributed to surface heterogeneity. A linearized Freundlich equation for aqueous solution is given as

$$\log q_e = \log k_f + \frac{1}{n}\log C_e$$

Where, k_f indicates adsorption capacity and n represents the adsorption intensity. The values of k_f ($mg^{1-1/n}L^{1/n}\,g^{-1}$) and n were obtained from the slope and intercept of the plot of log q_e versus log C_e, respectively (Fig 6b). The applicability of the isotherm equation was compared by evaluating the correlation coefficient (r^2). The correlation coefficient (r^2) values showed that adsorption data is well described by Langmuir adsorption isotherm model because correlation value is close to 1.0 for Langmuir adsorption isotherm (Table 1).

Kinetics study

The amount of metal ion adsorption by the adsorbent depends on the contact time and thus the study of the kinetics of adsorption is of considerable significance. The pseudo first order and pseudo second order kinetic models were employed to correlate the solid liquid adsorption. The pseudo first order kinetics is given by the equation

$$\log(q_e - q_t) = \log q_e - \frac{k_1 t}{2.303}$$

Where q_e (mg g^{-1}) and q_t (mg g^{-1}) refer to the amount adsorbed at equilibrium and at time t respective with the first order rate constant k_1 (min^{-1}). The plot of log (q_e-q_t) against time (min) gives pseudo first order rate constant with regression coefficient (Fig. 6c).

The pseudo second order equation is given as

$$\frac{t}{q_t} = \frac{1}{k_2 q_e} + \frac{t}{q_e}$$

Where k_2 is the pseudo second order rate constant in g mg^{-1} min^{-1} which can be obtained from the plot of t/q_t against time (min) (Fig. 6d). Among these two models, the pseuso-second order kinetics is followed by the adsorption process as revealed from the value of r^2 closer to 1[20-23].

Thermodynamics study

Effect of temperature on adsorption was studied in order to obtain relevant thermodynamic parameters at 300 K, 313 K, 323 K and 333 K. The free energy change of adsorption (ΔG^o) is related with the equilibrium constant K as

$$\Delta G^0 = -RT\ln K$$

van't Hoff equation which relates entropy (ΔS^o) and enthalpy (ΔH^o) changes are given by

$$\ln K = \frac{\Delta S^0}{R} - \frac{\Delta H^0}{RT}$$

Where R is gas constant, the values of ΔH^o and ΔS^o were obtained respectively from slope and intercept of the plot lnK against 1/T (Fig. 6e) as depicted in Table 2. The negative free energy change indicates the spontaneous nature, negative enthalpy change indicates exothermic nature of adsorption process while negative entropy change indicates the increase in randomness of fluoride ion as it passes from solution to adsorbed state.

Effect of co-existing ions

Water generally contained a series of chemical compositions that give a negative influence on defluoridation by adsorption process. So, it was very important to check the interference of co-existing ions on fluoride removal in binary solutions. The effect of assorted ions on defluoridation capacity was studied by using Zr-CTS beads with fixed initial concentration of 1 mM of co-ions like Cl^-, CO_3^{2-}, PO_4^{3-}, NO_3^- and SO_4^{2-} and same initial fluoride concentration. As shown in Fig 7a, the presence of diverse ion leads to detrimental effect on fluoride ion adsorption, resulting in decrease in fluoride removal efficiency. These may be due to competition among the anions to take the active sites on the surface of adsorbent which depends on concentration, size and charge on the anions[12]. Strong influence of

Table 1 — Adsorption Isotherm parameters

Isotherm	Parameters	Observations
Langmuir	q_o (mg g^{-1})	52.63
	b (L mg^{-1})	0.542
	r^2	0.983
Freundlich	k_f ($mg^{1-1/n}L^{1/n}\,g^{-1}$)	16.9
	n	2.67
	r^2	0.915

Table 2 — Thermodynamic parameters

Temperature (K)	ΔG^o (kJ mol^{-1})	ΔH^o (kJ mol^{-1})	ΔS^o (kJ mol^{-1} K^{-1})
303	-16.83	-12.62	0.014
313	-17.01		
323	-17.15		
333	-17.29		

Table 3 — Comparison table for fluoride adsorption on Zirconium modified chitosan composite and other reported materials

S. N.	Adsorbents	pH	Adsorption capacity (mg g^{-1})	Reference
1	Chitosan	6.0	1.39	24
2	Chitosan-Praseodymium complex	7.0	15.87	10
3	Rare Earth modified chitosan	5.0	3.72	25
4	Chitosan-Iron complex	3.0-10.0	2.34	26
5	Fabricated Chitosan Doped Graphite	6.5	37.9	27
6	Fe(III)- impregnated chitosan	7.0	20.75	28
7	Ti-chitosan spherical beads	7.0	7.2	29
8	La(III)-loaded bentonite/chitosan beads	5.0	2.87	11
9	Zr(IV) entrapped chitosan polymeric matrix	7.0	4.85	30
10	Ce(III)-incorporated crosslinked chitosan matrix	3.0	5.0	31
11	Chitosan-based magnetic nanocomposite	5.0	15.38	14
12	Zr(IV) immobilized crosslinked chitosan	6.0	48.26	15
13	Zr(IV)-Chitosan beads	4.0	52.63	Present work

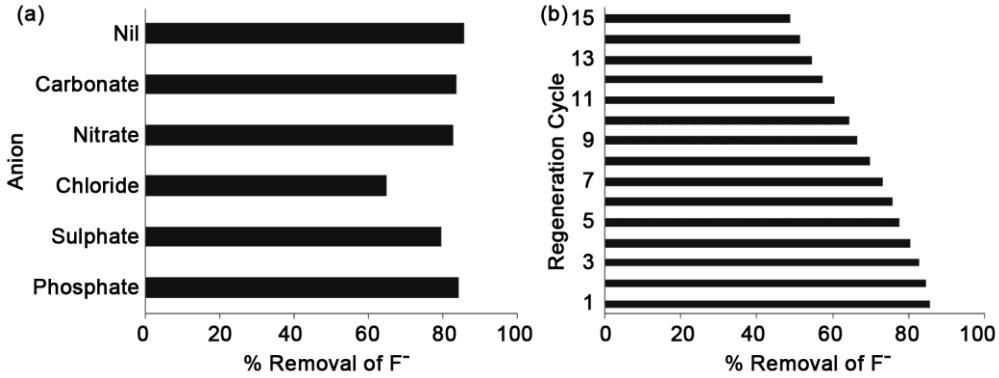

Fig. 7 — (a) Effect of co-existing ions and (b) adsorption cycles for regenerated Zr-CTS beads.

chloride ions on fluoride removal was observed, followed by sulphate and nitrate ions, while carbonate and phosphate had very little effect on defluoridation efficiency.

Reusability of composite studies

It is another important aspect to reapply or reuse the composite to evaluate its further adsorption property. For these, reagents such as NaCl, Na_2CO_3, Na_2SO_4 and $NaNO_3$ were examined for desorption studies. Among these, 5% (w/v) NaCl solution showed best results for desorption. The NaCl solution results into waning of electrostatic interaction between Zr(IV) chitosan composite and fluoride ions leading to desorption of fluoride ions. The percentage removal of fluoride was found to reduce from 84.6 % to 82.7% and 80.4% in two regenerations. After second regeneration, it reduced to less than 80% and dropped down to 49% in fifteenth cycle (Fig. 7b). Comparative results of defluoridation on natural chitosan and their

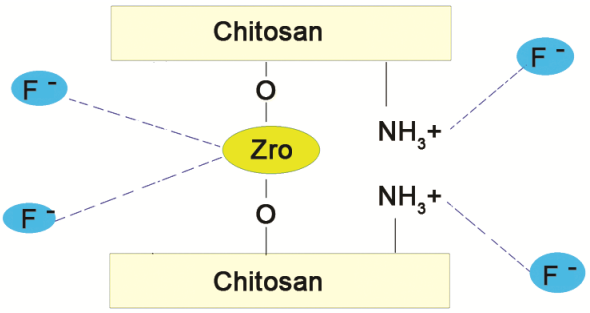

Fig. 8 — Schematic representation for the interaction of fluoride with Zr-CTS beads.

derivatives for different materials reported in literature are shown in Table 3. The comparison is self-explanatory and proves the ability of the material in comparison with earlier reported materials. The probable mechanism of adsorption can be explained on the basis of electrostatic interaction of F^- with Zr(IV) and with positively charged ammonium groups of chitosan at pH 4.0 (Fig. 8).

Conclusions

Zr-CTS beads have an excellent adsorption capacity of fluoride ion from aqueous solution. Physio-chemical characterization of these material expressed improved properties required for better adsorption for fluoride removal that one result led to 52.63 mg g^{-1} at pH 4.0 which indicates excellent and efficient removal of fluoride. The adsorption capacity was found to be much higher as compared to most of the reported materials. The adsorption process followed Freundlich adsorption isotherm in accordance with pseudo-second-order kinetics. Also the thermodynamic parameters showed that the removal process of fluoride by composite was exothermic. Negative free energy changes indicate the spontaneous process. The material was found to have easy synthesis process, cost effective and reusable in multiple cycles.

Acknowledgement

The authors are thankful to Department of Science and Technology, New Delhi for assistance under DST-FIST and RTM Nagpur University for university research project. One of the authors ST acknowledges BARTI, Pune for research fellowship.

References

1 Teotia S P S, Teotia M & Singh R K, *Fluoride*, 14 (1981) 69.
2 Kabata A & Pendias H, *Trace elements in soils and plants*, (CRC Press, Boca Raton, Florida), 1984, p 33431.
3 UNICEF State of the art report on the extent of fluoride in drinking water and the resulting endemicity in India., Report by Fluorosis Research & Rural Development Foundation for UNICEF, New Delhi (1999).
4 Ezzeddine A, Hannachi A & Bensalah N, *Desalin Water Treat*, 54 (2015) 2280.
5 Samadi M T, Zarrabi M, Sepehr M N, Ramhormozi S M, Azizian S & Amrane A, *Environ Eng Manag J*, 13 (2014) 205.
6 Xi B, Wang X, Liu W, Xia W, Li D, He L, Wang H, Sun W, Yang T & Tao W, *Sep Sci Technol*, 49 (2014) 2642.
7 Habuda-Stanić M, Ergović Ravančić M & Flanagan A, *Materials (Basel)*, 7 (2014) 6317.
8 Meenakshi S & Maheshwari R C, *J Hazard Mater*, B137 (2006) 456.
9 Gandhi R M, *J Bioremediat Biodegrad*, 7 (2016) 173.
10 Kusrini E, Sofyan N, Suwartha N, Yesya G & Priadi C R, *J Rare Earth*, 33 (2015) 1104.
11 Zhang Y, Xu Y, Cui H, Liu B, Gao X, Wang D & Liang P, *J Rare Earth*, 32 (2014) 458.
12 Shekhawat A, Kahu S S & Jugade R M, *RSC Adv*, 6 (2016) 18936.
13 Zhu T, Zhu T, Gao J, Zhang L & Zhang W, *J Fluor Chem*, 194 (2017) 80.
14 Abri A, Tajbakhsh M & Sadeghi A, *Water Supply*, 19 (2019) 40.
15 Liu Q, Zhanga L, Yang B & Huanga R, *Int J Biol Macromol*, 77 (2015) 15.
16 Sarkar D, Mohapatra D, Ray S, Bhattacharyya S, Adak S & Mitra N, *Ceram Int*, (2006) 1.
17 Prabhu S M, Elanchezhiyan S SD, Lee G & Meenakshi S, *Int J Biol Macromol*, 91 (2016) 1002.
18 Langmuir I, *J Am Chem Soc*, 40 (1918) 1361.
19 Freundlich H M F, Über *die adsorption in lösungen. Zeitschrift für Physikalische Chemie*, 57A (1906) 385.
20 Lagergren S., Zur theorie der sogenannten adsorption gelöster stoffe. Kungliga Svenska Vetenskaps-Akademiens. Handlingar, Band 24, Section II, No. 4 (1898) 1-39.
21 Ho Y S, *Scientometrics*, 59 (1) (2004) 171.
22 Ho & McKay G, *Chem Eng J*, 70 (2) (1998) 115.
23 Ho Y S, *J Hazard Mater*, 136 (3) (2006) 681-689.
24 Sahli Menkouchi M A, Annouar S, Tahaikt M, Mountadar M, Soufiane A & Elmidaoui A, *Desalin*, 212 (2007) 37.
25 Liang P, Zhang Y, Wang D, Xu Y & Luo L, *J Rare Earth*, 31 (2013) 817.
26 Patnaik S, Mishra P C, Nayak R N & Giri A K, *J Anal Bioanal Tech*, 79 (2016) 1-7.
27 Dongre R S, *Res. Develop Mater Sci*, 7 (2018) 1.
28 Zhang J, Chen N, Tang Z, Yu Y, Hu Q & Feng C, *Phys Chem Chem Phys*,17 (2015) 2.
29 Bansiwal A K, Thakre D, Labhshetwar N, Meshram S & Rayalu S, *Colloids Surf B*, 74 (2009) 216.
30 Viswananthan N & Meenakshi S, *Colloids Surf B*, 72 (2009) 88.
31 Li J, Liu Q, Hung R & Wang G, *J Rare Earth*, 34 (2016) 1053.